Clays Clay Miner., Vol. 71, No. 1:106–118, 2023
https://doi.org/10.1007/s42860-023-00236-6

ORIGINAL PAPER

The Formation and Transformation of Manganese Oxide Minerals on the Surface of Kaolinite

Fan Zhao · Guangyao Zhang · Yong Jiang · Hui Wang · Chi Cao · Yongbo Qi · Qingyun Wang · Huaiyan Zhao

Accepted: 10 May 2023 / Published online: 24 May 2023

Abstract The formation of manganese (Mn) oxides is influenced by environmental conditions and, in some red soils, Mn oxides occur as coatings on the surface of kaolinite particles in the form of colloidal films or fine particles. The present study aimed to explore the types of formation mechanisms of Mn oxide minerals on the surface of kaolinite. Mn oxide minerals synthesized by reducing the Mn in $KMnO_4$ with a divalent Mn salt ($MnSO_4$) were examined using X-ray diffraction (XRD) and scanning electron microscopy (SEM). The effects of various initial molar ratios of Mn^{2+}/Mn^{7+} (R = 1:0.67, 1:1, 1:2, and 1:4), cationic species (Na^+ or Mg^{2+}), synthesis temperatures (30, 60, and 110°C), and amount of added kaolinite (0.25, 0.5, 1.0, 2.0, and 5.0 g) on the formation of Mn oxides were studied. The results showed that Mn oxide mineral types were affected by the initial R value and the background cation. With decreases in the initial R value, the synthesized minerals transformed from cryptomelane to birnessite. The relative mass ratios of kaolinite to Mn oxide were calculated as 1:0.92, 1:0.63, 1:1.15, and 1:1.63. The sodium cation (Na^+) had a greater role than Mg^{2+} in promoting the dissolution–recrystallization of birnessite to cryptomelane. The synthesis temperature had no effect on mineral types, but Mn content increased as temperature increased. When the amount of added kaolinite was increased from 0.25 to 5.0 g, Mn oxide minerals formed gradually and transformed from birnessite to cryptomelane. This work revealed a possible formation process and reaction mechanism on the surface of kaolinite particles in some red soils.

Keywords Birnessite · Cationic species · Cryptomelane · Kaolinite · Mn^{2+}/Mn^{7+} molar ratios · Synthesis temperature

Associate Editor: William F. Jaynes

Supplementary Information The online version contains supplementary material available at https://doi.org/10.1007/s42860-023-00236-6.

F. Zhao · G. Zhang · Y. Jiang · C. Cao · Y. Qi · Q. Wang · H. Zhao (✉)
Anhui Province Key Lab of Farmland Ecological Conservation and Pollution Prevention, Key Laboratory of JiangHuai Arable Land Resources Protection and Eco-Restoration, College of Resources and Environment, Anhui Agricultural University, Hefei 230036, China
e-mail: huaiyanzhao@126.com

H. Wang
Soil and Fertilizer Institute, Anhui Academy of Agricultural Sciences, Hefei 230031, China

Introduction

Manganese is one of the major elements in the earth's crust and exists usually in the soil in the form of Mn oxide minerals due to weathering and pedogenesis (Hong et al., 2010; Huang et al., 2011; Namgung et al., 2018; Post, 1999). Mn oxide minerals are

ubiquitous in natural environments and are important components of soil (Huang et al., 2011). They are important sources of Mn for the nutrition of animals and plants, as well as one of the important adsorbents and carriers of environmental information (Huang et al., 2008, 2009; Villalobos et al., 2003). The high redox potential of Mn oxide minerals makes them active in the environment, so that they are used commonly as an important redox agent in the soil (Learman et al., 2011; Liu et al., 2020).

The formation and transformation of Mn oxide minerals in soil are influenced substantially by environmental changes and climate (Feng et al., 2004; Hong et al., 2010; Huang et al., 2011; Jung et al., 2020; McKenzie, 1971; Zhang et al., 2016). The crystallinity of Mn oxides in soil is low, and they are difficult to analyze and identify directly. Therefore, artificial laboratory simulation synthesis methods by reducing potassium permanganate with a divalent Mn salt were utilized to examine indirectly the formation mechanism of Mn oxide minerals. The product is fine-needle spherical crystals, which are very close to natural birnessite (Feng et al., 2004, 2005; Handel et al., 2013; Yang & Wang, 2002). Various kinds of Mn oxide minerals have been reported to have formed under different environmental conditions, such as the ratio of Mn^{2+}/MnO_4, the concentration of Mn^{2+}, temperature, background electrolyte, etc. (Cornell & Giovanoli, 1988; Handel et al., 2013; Hella et al., 2017; Kijima et al., 2001; Liang et al., 2020; Zhao et al., 2016; Zhu et al., 2010). The average oxidation states of Mn in birnessite are affected by the Mn^{2+}/MnO_4^- ratio and birnessite begins to form at low Mn^{2+}/MnO_4^- ratios (Luo et al., 1997). Furthermore, Ma et al. (2013) showed that synthetic Mn oxide minerals were transformed from cryptomelane to birnessite with a decrease in Mn^{2+}/MnO_4^- from 1:1 to 1:4. Mn^{2+} induced the transformation of birnessite to other new phases such as cryptomelane at room temperature (Tu et al., 1994). Background electrolytes affect the morphology, chemical composition, and crystal structure of birnessite (Zhang et al., 2018; Zhu et al., 2010). In the dissolution–recrystallization process of birnessite, todorokite was generated easily if the hydration ion radius of interlayer ions was large, such as Ca^{2+} and Mg^{2+}, while Mn oxides with smaller tunnel sizes such as cryptomelane were formed if the hydration ion radius was small, such as Na^+ and K^+ (Hella et al., 2017; Zhao et al., 2015). The dissolution-crystallization process was affected by temperature. Increasing the temperature shortened the induction period, increased the crystallization rate, and accelerated the phase transition from birnessite to other phases (Luo et al., 1997; Portehault et al., 2007).

The red soil region of southern China often undergoes periodic flooding in the rainy season due to high soil viscosity, poor drainage capacity, and mountainous and hilly landforms. With much rainfall and concomitant surface runoff in the rainy season, water accumulates and remains in low-lying areas, which leads to imperfect drainage and flooding. In the red soils of Guangxi, Guizhou, Fujian, etc., in particular, due to the geological and climatic factors listed above, the soils experience alternating oxidation/reduction conditions necessary for producing manganese oxide minerals. Therefore, the red soil of southern China is rich in Mn oxide minerals (Hong et al., 2010; Huang et al., 2008, 2009, 2011; Zhao et al., 2022). The hydrothermal conditions and redox potential of the soil affect significantly the formation, transformation, and surface properties of these Mn oxide minerals (Huang et al., 2011; Liang et al., 2020). Mn and Fe oxide minerals are often present simultaneously in red soils, where they are highly active (Chen et al., 2019; Huang et al., 2011; Krishnamurti & Huang, 1988; Liu et al., 2021; Luo et al., 2018). Iron oxide mineral surfaces can accelerate the oxidation of Mn(II) to form Mn oxides to a certain degree (Davies & Morgan, 1989). Iron oxide promoted significantly the oxidation of Mn^{2+} and crystallization of Mn oxide (Liu et al., 2022), which can be attributed to the fact that Fe oxide can function as a catalyst by promoting electron transfer between Mn^{2+} and dissolved O_2. The formation of manganite was catalyzed by the hematite surface which is explained by the electron transfer from adsorbed Mn(II) to another site with adsorbed O_2 via the band structure of the semiconducting hematite (Inoue et al., 2019). Semiconductor minerals (e.g. hematite, goethite, and ferrihydrite) show greater catalytic ability for Mn^{2+} oxidation than insulating minerals (e.g. albite, amorphous $Al(OH)_3$, and montmorillonite) (Lan et al., 2017). Furthermore, Mn oxide minerals are often coated or stored on the surface of kaolinite in the form of a colloidal film or as fine particles to form complexes (Choi et al., 2009; Khan et al., 2015; Mckenzie, 1972; Zhu et al., 2019). Kaolinite is also an insulating mineral, which may

https://doi.org/10.1007/s42860-023-00236-6 Published online by Cambridge University Press

provide a surface to precipitate the Mn mineral via heterogeneous nucleation. The formation and transformation of Fe oxide is significantly inhibited by the presence of kaolinite, while the presence of Fe^{2+} in solution accelerated it (Chen et al., 2019; Wei et al., 2011). Do Mn oxide minerals also form and transform on the surface of kaolinite? The factors which influence their formation and transformation have yet to be discovered.

In view of the above, the present study was performed in order to explore the types and formation mechanisms of Mn oxides synthesized on the surface of kaolinite, a typical mineral in red soil, considering the influencing factors of different Mn^{2+}/MnO_4^- molar ratios, cation types, synthesis temperature, and amount of kaolinite added. These results will provide a theoretical foundation for a better understanding of the formation process and reaction mechanism of Mn oxide in red soil and enrich the research of soil-interface chemistry.

Materials and Methods

Materials

Kaolinite was purchased from Sigma-Aldrich (Shanghai, China) Trading Co, Ltd (characterization of the kaolinite is described in the supplementary information), and $KMnO_4$ was acquired from Xilong Science Co., Ltd (Chengdu, China). $MnSO_4{\cdot}H_2O$, $MgSO_4$, and Na_2SO_4 were provided by Sinopharm Chemical Reagent Co., Ltd (Shanghai, China). Hydroxylamine hydrochloride was purchased from Aladdin Chemical Reagent Co., Ltd (Shanghai, China). All reagents were used without further purification. The HK-UV-10 (Hongke Technology Co., Ltd, Hefei, China) pure water purification system provided the deionized water (DDW) for this study.

Synthesis of Mn oxide Minerals on Kaolinite Surfaces

1 g of kaolinite was placed in a reactor containing 30 mL of 0.067, 0.1, 0.2, or 0.4 M $KMnO_4$ and 0.1 M Na_2SO_4 or $MgSO_4$. The reactor was placed in an oil bath at a specific temperature (30, 60, or 110°C) and at a stirring speed of 300 r/min. Then, 30 mL of 0.1 M $MnSO_4$ solution was added dropwise into the above-mixed solution using a peristaltic pump. This was followed by agitation of the mixtures for 30 min at constant temperature and aging for 24 h at 60°C after cooling (Frias et al., 2007). The aged minerals were centrifuged and cleaned with deionized water until the conductivity was < 20 μS cm^{-1}, then freeze-dried immediately, crushed, sieved with a 100-mesh sieve, and stored for further analysis. The synthesis conditions for all Mn oxides were the same.

Effect of the molar ratio of Mn^{2+} to Mn^{7+}

The Mn oxide minerals were synthesized at various molar ratios (R) of Mn^{2+} to Mn^{7+} (R = 1:0.67, 1:1, 1:2, and 1:4). The pH of the mixture was measured and found to be ~1.4. The synthesis temperature was controlled at 30°C, with Na^+ as the background cations. 1 g of kaolinite was added.

Effect of the background cations

The Mn oxide minerals were synthesized with the same concentrations of Na_2SO_4 or $MgSO_4$ as different background cations. 1 g of kaolinite was added at a synthesis temperature of 30°C. Meanwhile, a control experiment was conducted without background cations, and the other treatments were the same as above.

Effect of the synthesis temperature

The Mn oxide minerals were synthesized at 30, 60, and 110°C. The value of R was 1:4, with Na^+ as the background cation. 1 g of kaolinite was added.

Effect of the amount of kaolinite added

When the Mn oxide minerals were synthesized, the amount of kaolinite used was 0.25, 0.50, 1.0, 2.0, or 5.0 g. The value of R was 1:1, with a synthesis temperature of 30°C and Na^+ as the background cation. The synthesis procedure of Mn oxide minerals with various values of R was the same as above except that no kaolinite was added.

Mn content in Mineral Determinations

The synthetic kaolinite-Mn oxide mineral complex samples were dissolved by 0.25 M hydroxylamine

https://doi.org/10.1007/s42860-023-00236-6 Published online by Cambridge University Press

hydrochloride. The Mn contents of samples were measured using an A3AFG-13 (Purkinje General Instrument Co., Ltd, Beijing, China) flame atomic absorption spectrometer (Yan et al., 2020).

Relative Mass Ratio of Kaolinite to Mn oxide Determination

0.2 g of the sample was dissolved in 4 mL of 0.25 M hydroxylamine hydrochloride solution, which was placed in a 10 mL centrifuge tube, then centrifuged (8000 rpm, 10 min) and washed with deionized water. The supernatant was poured out and the residues of the samples after the dissolution were dried and weighed. This was the mass of kaolinite. The mass of Mn oxide was obtained from 0.2 g minus the mass of kaolinite. The relative mass ratio of kaolinite to Mn oxide in the final product was calculated (Neaman et al., 2004).

Characterization

X-ray diffraction (XRD)

The powder samples were characterized using an XD6 X-ray diffractometer (Purkinje General Instrument Co. Ltd., Beijing, China) using monochromatic CuKα radiation. The diffractometer was operated at a tube voltage of 36 kV and a tube current of 20 mA, and all of the XRD patterns of samples were scanned from 5 to 80°2θ at a scanning rate of 1°2θ per min.

Scanning electron microscopy (SEM)

The samples were mounted on sample holders with carbon glue and then gold coated. The samples were analyzed using the Zeiss Sigma 300 field emission scanning electron microscope (Oberkochen, Baden-Wurttemberg, Germany), with an accelerating voltage of 3 kV, and the microstructure and morphology of minerals were examined by SEM.

Results

Effect of the Molar Ratios of Mn^{2+} to Mn^{7+}

The Mn oxide minerals were synthesized on the surface of kaolinite by reducing potassium permanganate with a divalent Mn salt, controlling the molar ratios of Mn^{2+} to Mn^{7+} at 1:0.67, 1:1, 1:2, and 1:4 (Frias et al., 2007). In the system of adding kaolinite (Fig. 1), the synthesized kaolinite-Mn oxide complexes showed strong peaks of kaolinite (Choi et al., 2009). When R was 1:0.67, the complex also had characteristic diffraction peaks of cryptomelane and birnessite (Kijima et al., 2001; Tu et al., 1994; Zhao et al., 2016), indicating that the surface mineral of kaolinite was a mixture of cryptomelane and birnessite. However, when R was 1:1, the only Mn oxide on the surface of kaolinite was cryptomelane; when R was 1:2 and 1:4, Mn oxides formed were single-phase birnessite (Fig. 1a, b). The results showed, thus, that the types

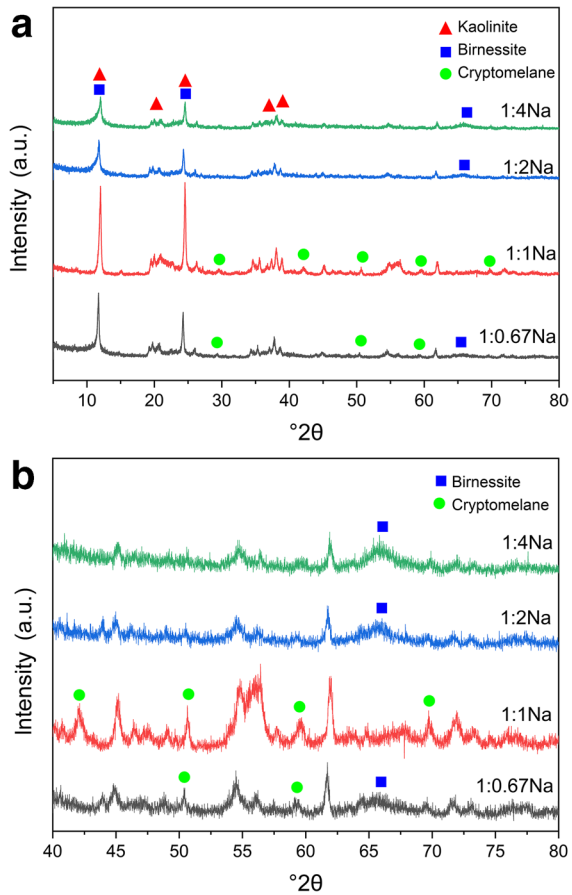

Fig. 1 XRD patterns of kaolinite-Mn oxide mineral complexes **a** with various molar ratios of Mn^{2+} to Mn^{7+} (R = 1:0.67, 1:1, 1:2, and 1:4); and **b** in the high-angle region. The synthesis temperature was controlled at 30°C, with Na^{+} as the background cation. 1 g of kaolinite was added. The labeled peaks are identified

https://doi.org/10.1007/s42860-023-00236-6 Published online by Cambridge University Press

of Mn oxides formed on the surface of kaolinite were influenced by the value of R.

Scanning electron microscopy images of the kaolinite-Mn oxide complexes with various R values and Na^+ as the background cation (Fig. 2) showed that kaolinite had a stacked-plate structure (Zhu et al., 2019). When R was 1:0.67, nanowire structures (diameter 0.2–2 μm; height 1–10 nm) and flower-spherical aggregate structures (formed by the flaky crystals (diameter 200–300 nm)) were formed on the surface of kaolinite (Fig. 2a). The nanowires structures and flower-spherical aggregate structures were the crystal morphology of cryptomelane and birnessite, respectively (Mckenzie, 1971; Portehault et al., 2007; Yin et al., 2018). When R was 1:1, the surface mineral of kaolinite was cryptomelane with nanowire structures (Fig. 2b). When R was 1:2 and 1:4, the surface minerals of kaolinite showed uniform flower-spherical aggregate structures (Fig. 2c, d), which was the crystal morphology of birnessite. The morphology changes shown by the SEM images were consistent with the mineral phase transformation results of the XRD patterns.

When the R values were 1:0.67, 1:1, 1:2, and 1:4, with Na^+ as the background cation, the Mn content in kaolinite-Mn oxide complexes was small, ~0.14, 0.10, 0.20, and 0.22 mg/g, respectively (Fig. 3). The Mn content among various treatments was significantly different ($P < 0.05$). In addition, the relative mass ratios of kaolinite to Mn oxide in the final product were calculated as 1:0.92, 1:0.63, 1:1.15, and 1:1.63. The mass percentage of Mn oxide in the final product increased when the R value decreased, except the sample with R = 1:1.

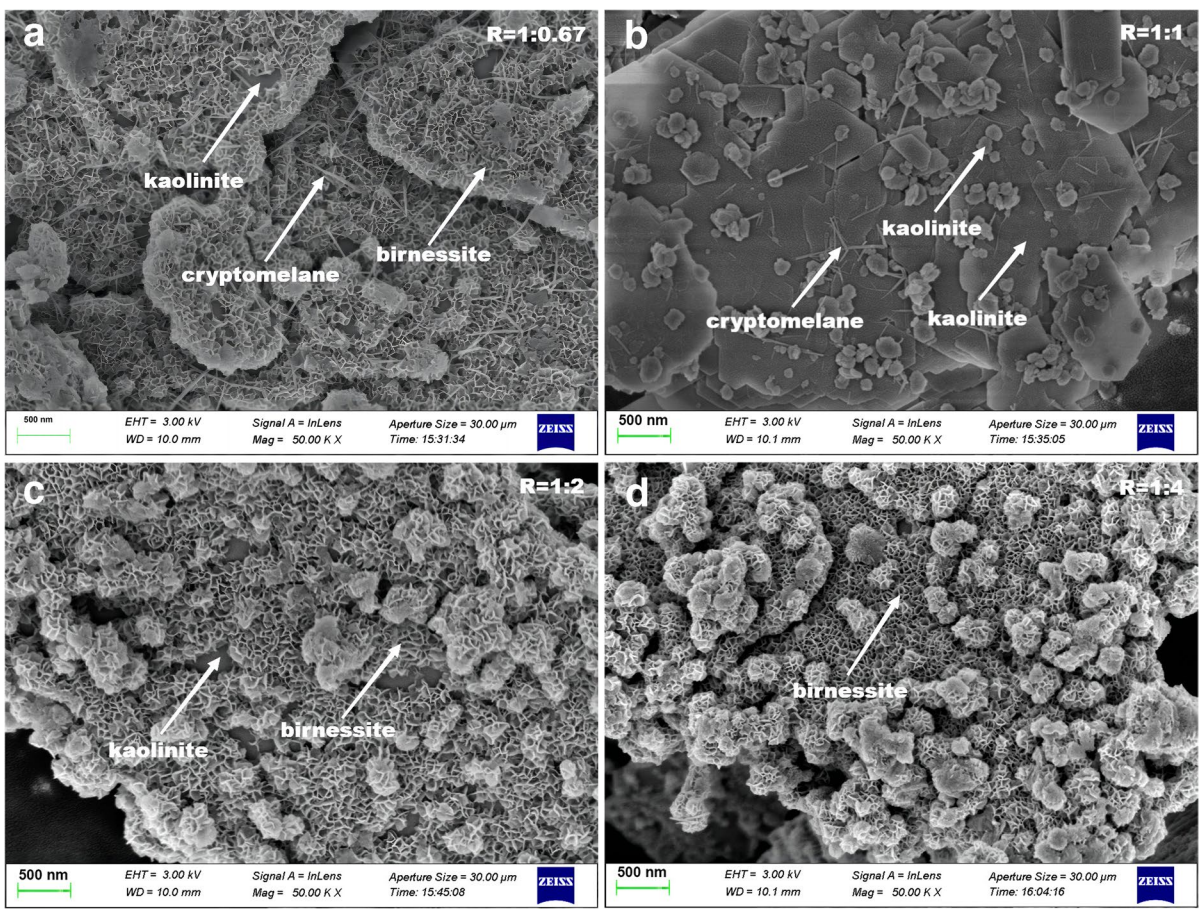

Fig. 2 SEM images of kaolinite-Mn oxide mineral complexes with Na^+ as the background cation; the R values were **a** 1:0.67, **b** 1:1, **c** 1:2, and **d** 1:4

https://doi.org/10.1007/s42860-023-00236-6 Published online by Cambridge University Press

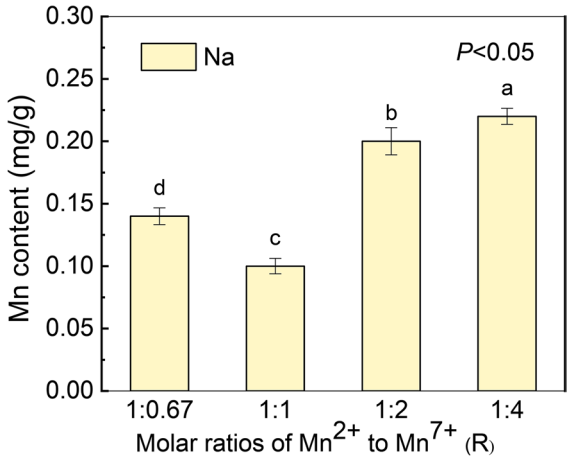

Fig. 3 Mn content in kaolinite-Mn oxide mineral complexes with Mn^{2+} to Mn^{7+} molar ratios of 1:0.67, 1:1, 1:2, and 1:4, with Na^{+} as the background cation

Effect of the Background Cation

The XRD pattern of kaolinite-Mn oxide complexes formed under the background cations of Na^{+}, Mg^{2+}, and without a background cation (Fig. 4) revealed that when R was 1:0.67, the characteristic peaks of cryptomelane and birnessite were both shown in complexes under different cation backgrounds, suggesting that the Mn oxide minerals synthesized on the surface of kaolinite were a mixture of cryptomelane and birnessite. When R was 1:2 and 1:4, the single-phase birnessite was synthesized under different cation backgrounds. However, when R was 1:1 with Na^{+} as the background cation (Fig. 1b), the complex had diffraction peaks characteristic of cryptomelane. Under Mg^{2+} as the background cation (Fig. 4a, c) and without a background cation (Fig. 4b, c), Mn oxides formed were composed of cryptomelane and birnessite. These results indicated that the presence of Na^{+} as the background cation promoted the transformation from birnessite to cryptomelane, while Mg^{2+} had no obvious effect.

When R was 1:0.67, 1:1, 1:2, and 1:4, the Mn contents of kaolinite-Mn oxide complexes with Na^{+} (Fig. 3) or Mg^{2+} (Fig. 5) as the background cation were 0.14, 0.10, 0.20, 0.22 mg/g and 0.14, 0.13, 0.18, 0.20 mg/g, respectively. The relative mass ratios of kaolinite to Mn oxides in the complexes were 1:0.92, 1:0.63, 1:1.15, 1:1.63 and 1:0.81, 1:0.67, 1:1.09, 1:1.53, respectively. This indicated that the Mn content of minerals on the surface of kaolinite was affected by the choice of background cation, although the difference was small. The Mn content and the mass percentage of Mn oxide in the final product with Na^{2+} as the background cation were generally larger than with Mg^{2+}.

Effect of the Temperature of Synthesis

From the analysis above, the mineral on the surface of kaolinite under different background cations with an R value of 1:4 was pure phase birnessite (Fig. 4), which is the most abundant Mn oxide mineral in the soil (Feng et al., 2004).

The effect of temperature on the formation of Mn oxides with an R value of 1:4 was studied. The kaolinite-Mn oxide complexes were synthesized at 30, 60, and 110°C. The XRD patterns (Fig. 6) revealed that, besides the characteristic diffraction peaks of kaolinite, there were very obvious peaks of birnessite at various temperatures (Fig. 6a, b), indicating that single-phase birnessite formed on the surface of kaolinite at various temperatures and temperature had no effect on the type of Mn oxide formed.

The Mn contents of kaolinite-Mn oxide complexes synthesized at 30, 60, and 110°C in Na^{+} (Fig. 7a) and Mg^{2+} (Fig. 7b) were 0.22, 0.28, 0.29 mg/g and 0.20, 0.27, 0.28 mg/g, respectively. The relative mass ratios of kaolinite to Mn oxide were 1:1.63, 1:2.14, 1:2.46, and 1:1.53, 1:1.87, 1:2.20, respectively. The results showed that the Mn content and the mass percentage of Mn oxide in complexes increased gradually with increase in temperature. The amount of birnessite on the surface of kaolinite increased gradually with increasing temperature.

Effect of Kaolinite Addition

Two different pretreatments were used, one without kaolinite (Fig. 8a) and the other with 0.25, 0.5, 1.0, 2.0, and 5.0 g of kaolinite added (Fig. 8b). With no added kaolinite the XRD pattern of Mn oxide showed that, when R was 1:0.67, only the characteristic diffraction peaks of cryptomelane were present. When R was 1:1, 1:2, and 1:4, the Mn oxide was birnessite (Fig. 8a). In the treatment with added kaolinite, when R was 1:1 and the amount of kaolinite was 0.25 or 0.50 g, the Mn oxide formed was birnessite. However, when 1.0, 2.0, or 5.0 g

https://doi.org/10.1007/s42860-023-00236-6 Published online by Cambridge University Press

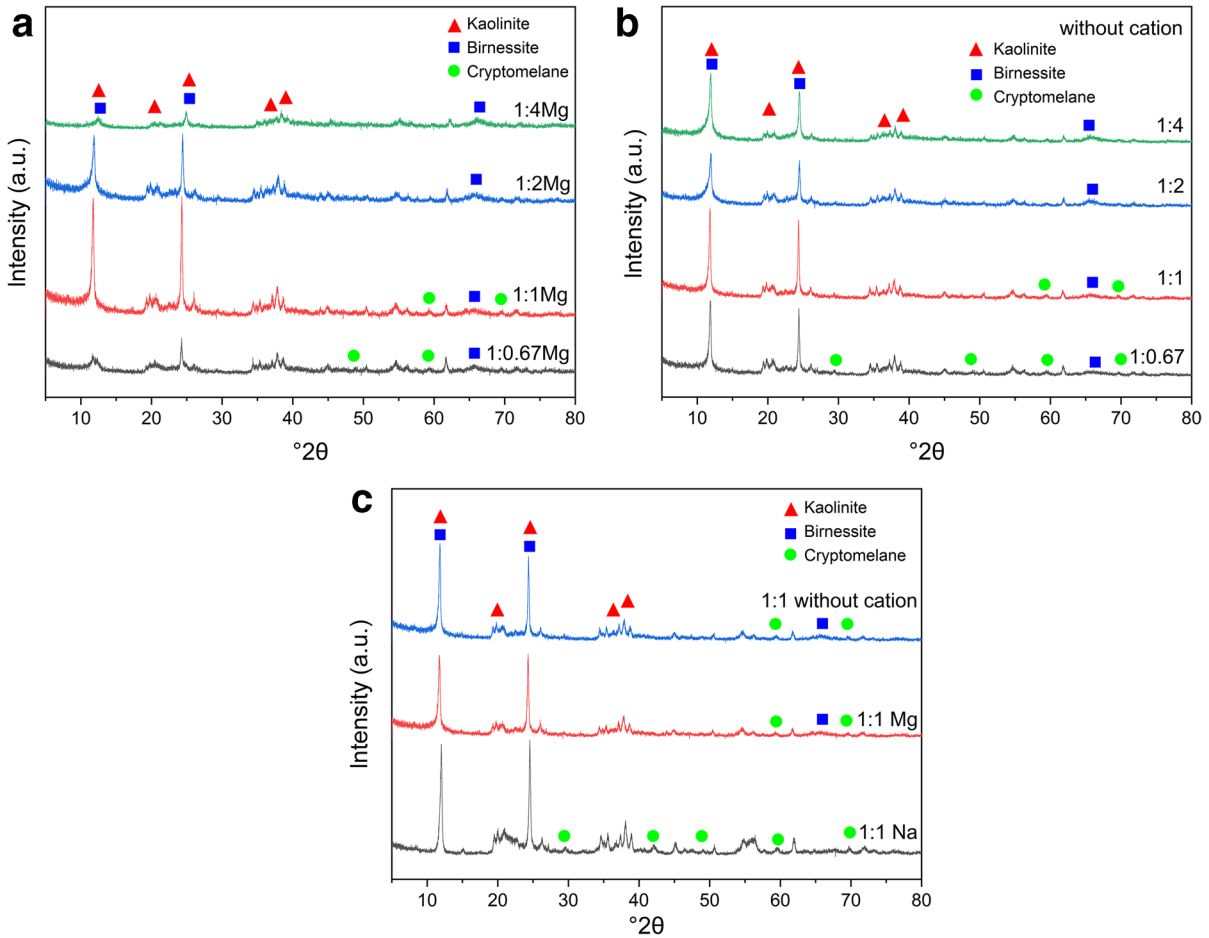

Fig. 4 XRD patterns of products formed after treatment of kaolinite-Mn oxide complex **a** with background Mg^{2+}cations; **b** without background cations; and **c** with background cations of Na^{+}, Mg^{2+}, and without background cations. The R value was 1:1. The labeled peaks are identified

of kaolinite was added, the Mn oxide formed was cryptomelane (Fig. 8b). In addition, the relative mass ratio of kaolinite and Mn oxide in the end products was calculated as 1:4.67, 1:2.34, 1:0.63, 1:0.53, and 1:0.28, for 0.25, 0.5, 1.0, 2.0, and 5.0 g of added kaolinite, respectively. With the increase in kaolinite content, the mass percentage of Mn oxide in the complex decreased gradually, which is also the reason why the diffraction peak intensity of kaolinite gradually became strong and sharp with the addition of kaolinite from 0.25 g to 5 g. The results showed that the addition of kaolinite affected the Mn oxide mineral type of the complexes; with increase in kaolinite concentration, the conversion rate of birnessite increased gradually, indicating that kaolinite can promote the process of birnessite dissolution and recrystallization into cryptomelane.

Discussion

The types of Mn oxide minerals were affected by various environmental conditions in the synthesis process. In the present study, birnessite and cryptomelane were synthesized under different molar ratios of Mn^{2+} to Mn^{7+} on the surface of kaolinite. The formation of birnessite on the surface of kaolinite followed one of two processes, and the chemical reaction stoichiometry of which was (Villalobos et al., 2003):

https://doi.org/10.1007/s42860-023-00236-6 Published online by Cambridge University Press

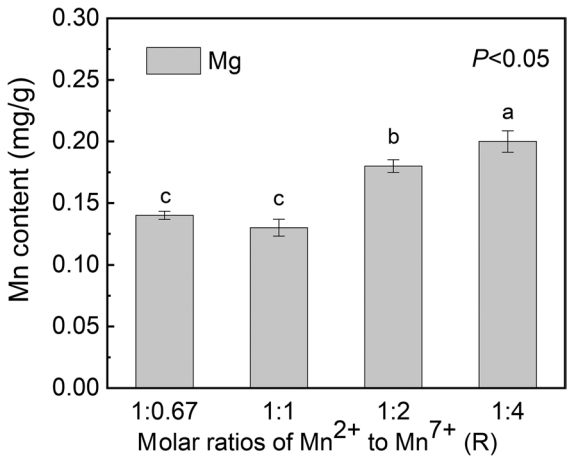

Fig. 5 Mn content in kaolinite-Mn oxide mineral complexes with Mn^{2+} to Mn^{7+} molar ratios of 1:0.67, 1:1, 1:2, and 1:4, with Mg^{2+} as the background cation

$$2\ MnO_4^- + 3\ Mn^{2+} + 2\ H_2O \rightarrow 5\ MnO_2\ (Birnessite) + 4\ H^+ \quad (1)$$

$$4\ MnO_4^- + 4\ H^+ \rightarrow 4\ MnO_2\ (Birnessite) + 2H_2O + 3\ O_2 \quad (2)$$

Studies have shown that the transformation of birnessite into cryptomelane is a process of dissolution–recrystallization (Lefkowitz et al., 2013; Zhang et al., 2011), and the interaction between birnessite and Mn^{2+} in solution promotes the transformation of birnessite (Morgan, 2005; Tu et al., 1994; Zhang et al., 2011). When R was 1:0.67 or 1:1, with gradual dropwise addition of of Mn^{2+}, the MnO_4^- in the system was exhausted gradually. With continuous dropwise addition of acidic Mn^{2+}, the acidity in the system was relatively strong and promoted the dissolution process and accelerated recrystallization. The dissolution of birnessite and the recrystallization of Mn oxide octahedra continued in the system until birnessite was dissolved completely and transformed into cryptomelane (Zhang et al., 2011; Zhao et al., 2015). When R was 1:0.67, the reaction was in the process of dissolution–recrystallization, a mixture of birnessite and cryptomelane was formed. When R was 1:1, and the reaction completed, birnessite was converted into cryptomelane completely. When R was 1:2 and 1:4, the concentration of MnO_4^- in the system was greater, and Mn^{2+} was consumed completely in the reaction system, and the product was single-phase birnessite (Tu et al., 1994). The Mn oxide mineral

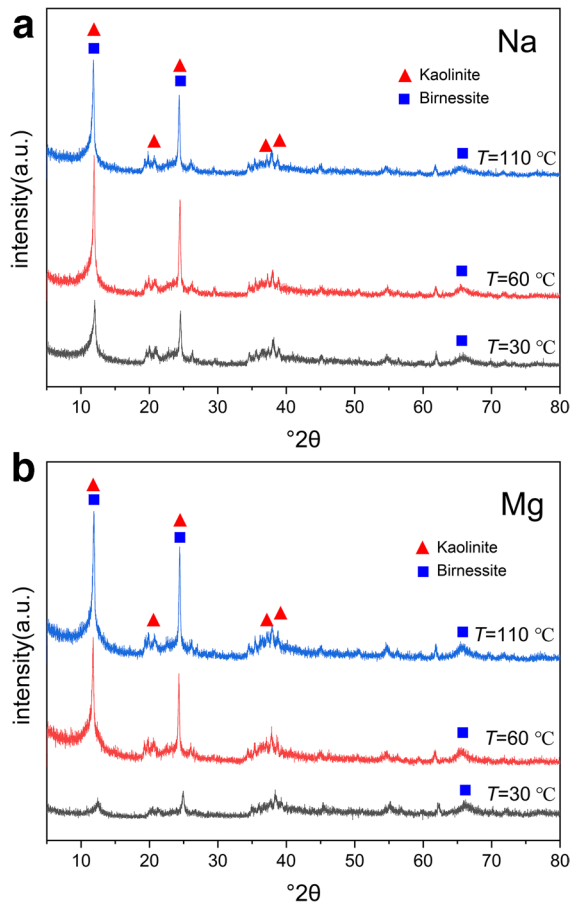

Fig. 6 XRD patterns of kaolinite-Mn oxide mineral complexes formed with R = 1:4 and with 1 g of added kaolinite; the synthesis temperatures were 30, 60, and 110°C, with background **a** Na^+ and **b** Mg^{2+} cations. The labeled peaks are identified

types on the surface of kaolinite transformed from the mixture of birnessite and cryptomelane to birnessite as the R value decreased within a certain R value range, which was consistent with the results reported by Ma et al. (2013). The R value affects directly the type of Mn oxide synthesized. In addition, the coating amount of Mn oxide in the complexes was also affected by the R value. When the R value decreased, the amount of Mn in minerals increased, which may be related to the crystallinity of the Mn oxide minerals. When the crystallization of Mn oxide minerals was weaker, the mineral crystals formed were smaller and the effective area in contact with the kaolinite increased, thus more easily covering the kaolinite surface (Khan et al., 2015). Furthermore, as the R value

https://doi.org/10.1007/s42860-023-00236-6 Published online by Cambridge University Press

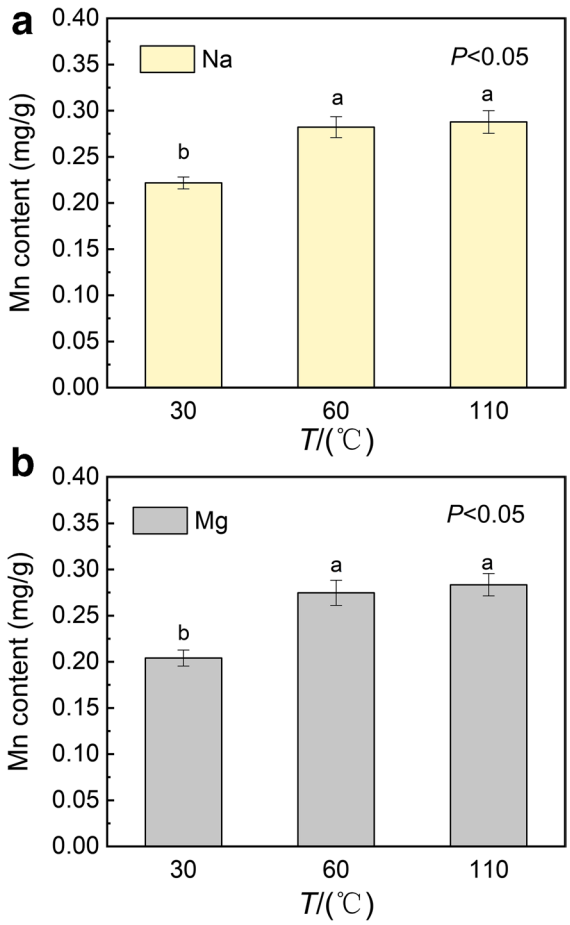

Fig. 7 Mn content in kaolinite-Mn oxide minerals under the background of **a** Na^+, **b** Mg^{2+} at 30, 60, and 110°C, with the R value = 1:4 and the amount of kaolinite added was 1 g

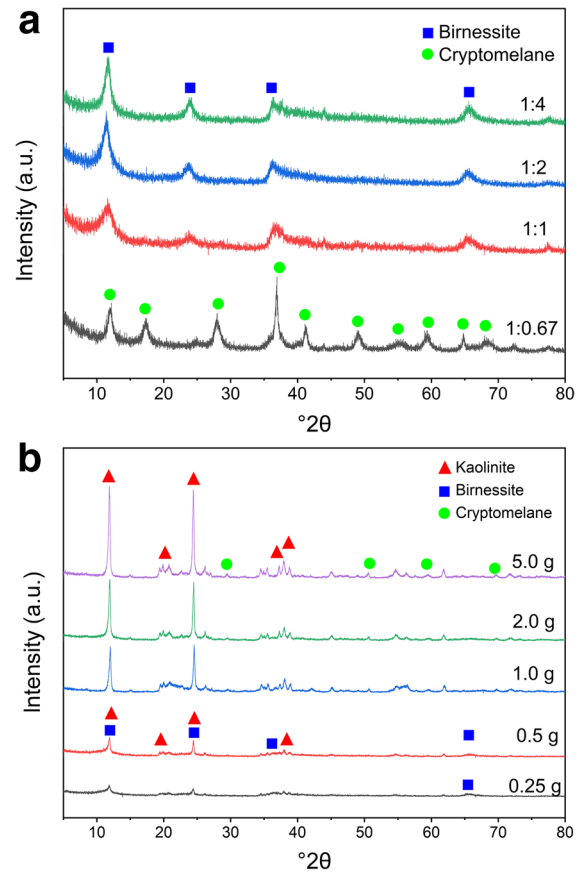

Fig. 8 XRD patterns of **a** Mn oxide minerals and **b** kaolinite-Mn oxide mineral complexes formed when using the following amounts of kaolinite: 0.25, 0.5, 1.0, 2.0, and 5.0 g, with Na^+ as the background cation; the value of R was 1:1; the synthesis temperature was 30°C

decreased, the concentration of MnO_4^- in the system increased, the reaction between excess MnO_4^- in the solution and H^+ formed more birnessite (chemical reaction process 2). The amount of Mn in minerals increased accordingly (Zhang et al., 2011). When the R value was 1:1, the amount of MnO_4^- in the system was insufficient (chemical reaction process 1). With continuous dropwise addition of Mn^{2+}, the birnessite transformed into cryptomelane through dissolution-recrystallization (Tu et al., 1994; Zhang et al., 2011). At this time, birnessite was in the stage of dissolution-recombination, and the Mn content in the complex was smaller than that in other conditions. This assumption was also confirmed by XRD studies. As seen in the XRD pattern (Fig. 1), when R was 1:1, the kaolinite peak was strongest, probably caused by the amount of Mn oxide synthesized on the kaolinite surface being least.

In addition, coexisting cations will also affect the type of Mn oxide. Studies have shown that coexisting cations can affect the layer structure, microstructure, and crystallinity of the Mn oxide, and a series of new minerals can be obtained from birnessite by ion exchange (Feng et al., 2004; Hella et al., 2017; Luo et al., 1997; Zhu et al., 2010). The interlayer Na^+ of birnessite has been shown (Zhao et al., 2015) to exchange easily with Mg^{2+}, which indicates that the structure of birnessite with Mg^{2+} as the interlayer ion is more stable. The hydrated ionic radius of Na^+ (3.58 Å) is less than Mg^{2+} (4.28 Å) (Kuma et al., 1994; Zhang et al., 2018), so Mg^{2+} with a larger radius (relative to Na^+) prevents the structural

https://doi.org/10.1007/s42860-023-00236-6 Published online by Cambridge University Press

layer of birnessite from collapsing (Feng et al., 2005; Zhang et al., 2016, 2018). The hydrated ionic radius of Na^+ was too small to support the layered structure of birnessite in the process of dissolution–recrystallization, and the interlayer space of 0.72 nm in birnessite collapses easily. Finally, the cryptomelane with a tunnel structure was formed (Zhang et al., 2011). Therefore, when the R value was 1:1, the single-phase cryptomelane was synthesized with Na^+ as the background cation. However, with Mg^{2+} as the background cation, the surface mineral of kaolinite was a mixture of cryptomelane and birnessite. The amount of Mn oxide synthesized under various background cations differs slightly. The Mn content when Mg^{2+} was the background cation$^+$ was generally smaller than in the background cations of Na^+, which may be attributed to the delayed crystallization rate of the system with Mg^{2+}. Birnessite crystallization occurs in three stages: an induction period, a fast crystallization period, and a steady-state period (Luo et al., 1997). The induction period with Mg^{2+} was longer than that of the Mg^{2+} free synthesis; thus, the amount of Mn was smaller with the coexisting Mg^{2+}.

Increasing the temperature can shorten the induction period and increase the crystallization rate (Luo et al., 1997). In the present study, only birnessite formed on the surface of kaolinite over the temperature range 30 to 110°C. This suggested that increasing the temperature within a certain temperature range (30–110°C) was conducive to the formation of birnessite on the surface of kaolinite. The temperature affected the Mn content in minerals; the Mn content in complexes increased gradually with increasing temperature (Fig. 7).When the temperature was low, the crystallinity of birnessite was obviously impeded, while high temperature accelerated the crystallization rate (Luo et al., 1997). As a result, birnessite formed quickly and had a larger Mn content at higher temperature.

Mn oxides in soil are not only observed commonly in nodules containing high concentrations of the oxides of Fe and Mn, but also often occur coated or stored on the surface of clay minerals such as kaolinite in the form of colloidal films or fine particles (Choi et al., 2009; Khan et al., 2015; Liu et al., 2021; McKenzie, 1972). Studies have shown that mineral surfaces, such as Fe (oxyhydr)oxides, can accelerate the oxidation of Mn^{2+} to form Mn oxides to a certain degree (Jung et al., 2020, 2021; Lan et al., 2017). Kaolinite is an insulating mineral, which may provide a surface on which to precipitate the Mn oxides via heterogeneous nucleation. SEM images (Fig. 2) demonstrated the uniform distribution of birnessite/cryptomelane on the surface of kaolinite. This is similar to a previous report (Won et al., 2020) which showed that kaolinite particles may play a role as nucleation sites and promote the heterogeneous nucleation of calcite.

Conclusions

The Mn oxide minerals formed on the surface of kaolinite particles were affected by the initial molar ratio of Mn^{2+} to Mn^{7+} (R). When R was 1:0.67, the product contained both birnessite and cryptomelane, while when R was 1:1, the product was single-phase cryptomelane, and single-phase birnessite was formed when R was 1:2 and 1:4. As the R value was decreased, the Mn content in the minerals increased. Background cations also affected the type of Mn oxide formed on the surface of kaolinite. The Na^+ ion promoted birnessite transformation by dissolution/recrystallization to cryptomelane, while Mg^{2+} had no obvious effect. Furthermore, the Mn content in the background Mg^{2+} cation solution was generally less than in the Na^+ solution. The synthesis temperature had no effect on the type of Mn oxide mineral formed, but Mn content increased as the temperature was increased. When the amount of kaolinite added was increased from 0.25 to 5.0 g, the Mn oxide minerals synthesized were transformed gradually from birnessite to cryptomelane. With an increase in kaolinite content, the relative mass ratios of kaolinite to Mn oxide in the end products was calculated as 1:4.67, 1:2.34, 1:0.63, 1:0.53, and 1:0.28.

Acknowledgements The authors acknowledge the support of Anhui Province Key Lab of Farmland Ecological Conservation and Pollution Prevention, the Opening Fund Project of National Red Soil Improvement Engineering Technology Research Center (Grant No. 2020NETRCRSI-13). The authors are also grateful to the Editor-in-Chief and the anonymous reviewers for their very helpful comments and suggestions.

Authors' Contributions Authors whose names appear on the submission were involved in the writing and revision of the manuscript. All authors have contributed equally to the work.

Funding Sources are as stated in the Acknowledgments.

Data Availability All data are contained within the article.

Code Availability Not applicable.

Declarations

The manuscript has not been submitted to more than one journal for simultaneous consideration and has not been published in full or in part previously. Compliance with ethical statements and all authors consent to participate.

Consent for Publication All authors give consent for publication.

Conflict of Interest The authors declare that they have no conflict of interest.

References

Chen, H. F., Koopal, L. K., Xu, J. L., Wang, M. X., & Tan, W. F. (2019). Selective adsorption of soil humic acid on binary systems containing kaolinite and goethite: Assessment of sorbent interactions. *European Journal of Soil Science, 70*(5), 1098–1107.

Choi, J., Komarneni, S., & Park, M. (2009). Mn-kaolinite synthesis under low-temperature hydrothermal conditions. *Applied Clay Science, 44*(3–4), 237–241.

Cornell, R. M., & Giovanoli, R. (1988). Transformation of hausmannite into birnessite in alkaline media. *Clays and Clay Minerals, 36*, 249–257.

Davies, S. H. R., & Morgan, J. J. (1989). Manganese(II) oxidation kinetics on metal oxide surfaces. *Journal of Colloid and Interface Science, 129*(1), 63–77.

Feng, X. H., Liu, F., Tan, W. F., & Liu, X. W. (2004). Synthesis of birnessite from the oxidation of Mn^{2+} by O_2 in alkali medium: Effects of synthesis conditions. *Clays and Clay Minerals, 52*(2), 240–250.

Feng, X. H., Tan, W. F., Liu, F., Huang, Q. Y., & Liu, X. W. (2005). Pathways of birnessite formation in alkali medium. *Science China Earth Sciences, 48*(9), 1438–1451.

Frias, D., Nousir, S., Barrio, I., Montes, M., Lopez, T., Centeno, M. A., & Odriozola, J. A. (2007). Synthesis and characterization of cryptomelane-type and birnessite-type oxides: Precursor effect. *Materials Characterization, 58*(8–9), 776–781.

Handel, M., Rennert, T., & Totsche, K. U. (2013). Synthesis of cryptomelane-type and birnessite-type manganese oxides at ambient pressure and temperature. *Journal of Colloid and Interface Science, 405*, 44–50.

Hella, B., Romain, C., Ghouti, M., Christian, R., & Latifa, B. (2017). Conditions for the formation of pure birnessite during the oxidation of Mn(II) cations in aqueous alkaline medium. *Journal of Solid State Chemistry, 248*, 18–25.

Hong, H. L., Gu, Y. S., Yin, K., Zhang, K. X., & Li, Z. H. (2010). Red soils with white net-like veins and their climate significance in south China. *Geoderma, 160*(2), 197–207.

Huang, L., Hong, J., Tan, W. F., Hu, H. Q., Liu, F., & Wang, M. K. (2008). Characteristics of micromorphology and element distribution of iron-manganese cutans in typical soils of subtropical China. *Geoderma, 146*(1–2), 40–47.

Huang, L., Tan, W. F., Liu, F., Hu, H. Q., & Wang, M. K. (2009). Characteristics of iron-manganese cutans and matrices in Alfisols and Ultisols of subtropical China. *Soil Science, 174*, 238–246.

Huang, C. Q., Zhao, W., Liu, F., Tan, W. F., & Koopal, L. K. (2011). Environmental significance of mineral weathering and pedogenesis of loess on the southernmost Loess Plateau. *China. Geoderma, 163*(3–4), 219–226.

Inoue, S., Yasuhara, A., Ai, H., Hochella, M. F., & Murayama, M. (2019). Mn(II) oxidation catalyzed by nanohematite surfaces and manganite/hausmannite core-shell nanowire formation by self-catalytic reaction. *Geochimica et Cosmochimica Acta, 258*, 79–96.

Jung, H., Taillefert, M., Sun, J., Wang, Q., Borkiewicz, O. J., Liu, P., Yang, L. F., Chen, S., Chen, H. L., & Tang, Y. Z. (2020). Redox cycling driven transformation of layered manganese oxides to tunnel structures. *Journal of the American Chemical Society., 142*, 2506–2513.

Jung, H., Xu, X. M., Wan, B., Wang, Q., Borkiewicz, O. J., Li, Y., Chen, H. L., Lu, A. H., & Tang, Y. Z. (2021). Photocatalytic oxidation of dissolved Mn(II) on natural iron oxide minerals. *Geochimica et Cosmochimica Acta, 312*, 343–356.

Khan, T. A., Khan, E. A., & Shahjahan. (2015). Removal of basic dyes from aqueous solution by adsorption onto binary iron-manganese oxide coated kaolinite: Non-linear isotherm and kinetics modeling. *Applied Clay Science, 107*, 70–77.

Kijima, N., Yasuda, H., Sato, T., & Yoshimura, Y. (2001). Preparation and characterization of open tunnel oxide α-MnO_2 precipitated by ozone oxidation. *Journal of Solid State Chemistry, 159*, 94–102.

Krishnamurti, G. S. R., & Huang, P. M. (1988). Influence of manganese oxide minerals on the formation of iron oxides. *Clays and Clay Minerals, 36*, 467–475.

Kuma, K., Usui, A., Paplawsky, W., Gedulin, B., & Arrhenius, G. (1994). Crystal structures of synthetic 7 angstrom and 10 angstrom manganates substituted by mono- and divalent cations. *Mineralogical Magazine, 58*(4), 425–447.

Lan, S., Wang, X. M., Xiang, Q. J., Yin, H., Tan, W. F., Qiu, G. H., Zhang, J., & Feng, X. H. (2017). Mechanisms of Mn(II) catalytic oxidation on ferrihydrite surfaces and the formation of manganese (oxyhydr)oxides. *Geochimica et Cosmochimica Acta., 211*, 79–96.

Learman, D. R., Voelker, B. M., Rodriguez, V. A. I., & Hansel, C. M. (2011). Formation of manganese oxides by bacterially generated superoxide. *Nature Geoscience, 4*(2), 95–98.

Lefkowitz, J. P., Rouff, A. A., & Elzinga, J. E. (2013). Influence of pH on the reductive transformation of birnessite by aqueous Mn(II). *Environmental Science & Technology, 47*(18), 10364–10371.

Liang, X. R., Post, J. E., Lanson, B., Wang, X. M., Zhu, M. Q., Liu, F., Tan, W. F., Feng, X. H., Zhu, G. M., Zhang, X., & De Yoreo, J. J. (2020). Coupled morphological and structural evolution of δ-MnO_2 to α-MnO_2 through multistage oriented assembly processes: The role of Mn(III). *Environmental Science: Nano, 7*, 238–249.

Liu, J., Zhang, Y. X., Gu, Q., Sheng, A. X., & Zhang, B. G. (2020). Tunable Mn oxidation state and redox potential of birnessite coexisting with aqueous Mn(II) in mildly acidic environments. *Minerals, 10*(8), 690.

Liu, J., Sayako, I., Zhu, R. L., He, H. P., & Hochella, M. F., Jr. (2021). Facet-specific oxidation of Mn (II) and heterogeneous growth of manganese (oxyhydr) oxides on hematite nanoparticles. *Geochimica Et Cosmochimica Acta, 307*, 151–167.

Liu, J., Chen, Q., Yang, Y., Wei, H., Laipan, M., Zhu, R., He, H. P., & Hochella, M. F. (2022). Coupled redox cycling of Fe and Mn in the environment: The complex interplay of solution species with Fe- and Mn-(oxyhydr)oxide crystallization and transformation. *Earth-Science Reviews, 232*, 104105.

Luo, J., Steven, L., & Suib. (1997). Preparative parameters, magnesium effects, and anion effects in the crystallization of birnessites. *Journal of Physical Chemistry B, 101*, 10403–10413.

Luo, Y., Ding, J., Shen, Y., Tan, W. F., Qiu, G., & Liu, F. (2018). Symbiosis mechanism of iron and manganese oxides in oxic aqueous systems. *Chemical Geology, 488*, 162–170.

Ma, G., Liu, F., Huang, L., & Sun, M. M. (2013). The process and influence factors of the synthesis of manganese minerals by the reactions between $KMnO_4$ and bivalent manganese salts. *Acta Petrologica Et Mineralogica, 32*(03), 393–400. https://doi.org/10.3969/j.issn.1000-6524.2013.03.011

McKenzie, R. M. (1971). The synthesis of birnessite, cryptomelane, and some other oxides and hydroxides of manganese. *Mineralogical Magazine, 38*, 493–502.

McKenzie, R. M. (1972). The manganese oxides in soils—a review. *Journal of Plant Nutrition and Soil Science, 131*(3), 221–242. https://doi.org/10.1002/jpln.19721310302

Morgan, J. J. (2005). Kinetics of reaction between O_2 and Mn(II) species in aqueous solutions. *Geochimica et Cosmochimica Acta, 69*(1), 35–48.

Namgung, S., Chon, C. M., & Lee, G. (2018). Formation of diverse Mn oxides: A review of bio-geochemical processes of Mn oxidation. *Geosciences Journal, 22*(2), 373–381.

Neaman, A., Waller, B., Mouele, F., Trolard, F., & Bourrie, G. (2004). Improved methods for selective dissolution of manganese oxides from soils and rocks. *European Journal of Soil Science, 55*(1), 47–54.

Portehault, D., Cassaignon, S., Baudrin, E., & Jolivet, J. P. (2007). Morphology control of cryptomelane type MnO_2 nanowires by soft chemistry, growth mechanisms in aqueous medium. *Chemistry of Materials, 19*(22), 5410–5417.

Post, J. E. (1999). Manganese oxide minerals: Crystal structures and economic and environmental significance. *Proceedings of the National Academy of Sciences of the United States of America, 96*(7), 3447–3454.

Tu, S., Racz, G. J., & Goth, T. B. (1994). Transformations of synthetic birnessite as affected by pH and manganese concentration. *Clays and Clay Minerals, 42*, 321–330.

Villalobos, M., Toner, B., Bargar, J., & Sposito, G. (2003). Characterization of the manganese oxide produced by Pseudomonas putida strain *MnB1*. *Geochimica Et Cosmochimica Acta, 67*(14), 2649–2662.

Wei, S. Y., Liu, F., Feng, X. H., Tan, W. F., & Koopal, L. K. (2011). Formation and transformation of iron oxide-kaolinite associations in the presence of iron(II). *Soil Science Society of America Journal, 75*(1), 45–55.

Won, J., Jeong, B., Lee, J., Dai, S., & Burns, S. E. (2020). Facilitation of microbially induced calcite precipitation with kaolinite nucleation. *Geotechnique, 71*(8), 728–734.

Yan, C. L., Liu, S., Min, H., Li, C., Zhu, Z. X., Lu, C. S., & Gao, Q. (2020). Optimization and evaluation of the method for the determination of the manganese content in manganese ores and concentrates as described in ISO 4298:1984. *Analytical and Bioanalytical Chemistry, 412*(25), 6823–6831.

Yang, D. S., & Wang, M. K. (2002). Syntheses and characterization of birnessite by oxidizing pyrochroite in alkaline conditions. *Clays and Clay Minerals, 50*(1), 63–69.

Yin, H., Wang, X., Qin, Z., Vogel, M. G., Zhang, S., Jiang, S., Liu, F., Li, S., Zhang, J., & Wang, Y. (2018). Coordination geometry of Zn^{2+} on hexagonal turbostratic birnessites with different Mn average oxidation states and its stability under acid dissolution. *Journal of Environmental Sciences, 65*, 282–292.

Zhang, Q., Xiao, Z. D., Feng, X. H., Tan, W. F., Qiu, G. H., & Liu, F. (2011). Alpha-MnO_2 nanowires transformed from precursor delta-MnO_2 by refluxing under ambient pressure: The key role of pH and growth mechanism. *Materials Chemistry and Physics, 125*(3), 678–685.

Zhang, Q., Chen, X. D., Qiu, G. H., Liu, F., & Feng, X. H. (2016). Size-controlled synthesis and formation mechanism of manganese oxide OMS-2 nanowires under reflux conditions with $KMnO_4$ and inorganic acids. *Solid State Sciences, 55*, 152–158.

Zhang, T. F., Liu, L. H., Tan, W. F., Suib, S. L., Qiu, G. H., & Liu, F. (2018). Photochemical formation and transformation of birnessite: Effects of cations on micromorphology and crystal structure. *Environmental Science & Technology, 52*(12), 6864–6871.

Zhao, H. Y., Liang, X. R., Yin, H., Liu, F., Tan, W. F., Qiu, G. H., & Feng, X. H. (2015). Formation of todorokite from "c-disordered" H^+-birnessites: The roles of average manganese oxidation state and interlayer cations. *Geochemical Transactions, 16*, 8.

Zhao, H. Y., Zhu, M. Q., Li, W., Elzinga, E. J., Villalobos, M., Liu, F., Zhang, J., Feng, X. H., & Sparks, D. L. (2016). Redox reactions between Mn(II) and hexagonal birnessite change its layer symmetry. *Environmental Science & Technology, 50*, 1750–1758.

Zhao, F. F., He, M. C., Wang, Y. T., Tao, Z. G., & Li, C. (2022). Eco-geological environment quality assessment based on multi-source data of the mining city in red soil hilly region. *China. Journal of Mountain Science, 19*(1), 253–275.

Zhu, M. Q., Vogel, M. G., Parikh, S. J., Feng, X. H., & Sparks, D. L. (2010). Cation effects on the layer structure of

biogenic Mn-oxides. *Environmental Science & Technology, 44*, 4465–4471.

Zhu, B. L., Qi, C. L., Zhang, Y. H., Teresa, B., Xu, Z. H., Fan, Y. G., & Sun, Z. X. (2019). Synthesis, characterization and acid-base properties of kaolinite and metal (Fe, Mn, Co) doped kaolinite. *Applied Clay Science, 179*, 105138.

https://doi.org/10.1007/s42860-023-00236-6 Published online by Cambridge University Press